ACS APPLIED MATERIALS & INTERFACES

Research Article

www.acsami.org

# Self-Repairing Systems Based on Ionomers and Epoxidized Natural Rubber Blends

Md. Arifur Rahman,[†] Maurizio Penco,[†] Isabella Peroni,[†] Giorgio Ramorino,[†] Antonio Mattia Grande,[‡] and Luca Di Landro*[,‡]

[†]Department of Mechanical and Industrial Engineering, University of Brescia, Via Valotti 9, 25123 Brescia, Italy

[‡]Department of Aerospace Engineering, Polytechnic of Milan, via La Masa 34, 20156 Milano, Italy

**ABSTRACT:** The development of materials with the ability of intrinsic self-repairing after damage in a fashion resembling that of living tissues has important scientific and technological implications, particularly in relation to cost-effective approaches toward damage management of materials. Natural rubbers with epoxy functional groups in the macromolecular chain (ENR) and ethylene-methacrylic acid ionomers having acid groups partially neutralized with metal ions possess self-repairing behavior following high energy impacts. This research investigates the self-repairing behavior of both ENR and ionomers during ballistic puncture test on the basis of their thermal and mechanical properties. Heterogeneous blending of ionomers and ENR have also been used here as a strategy to tune the thermal and mechanical properties of the materials. Interestingly, blends of sodium ion containing ionomer exhibit complete self-repairing behavior, whereas blends of zinc ion containing ionomer show limited mending. The chemical structure studied by FTIR and thermal analysis shows that both ion content of ionomer and functionality of ENR have significant influence on the self-repairing behavior of blends. The mobility of rubbery phases along with its interaction to ionomer phase in the blends significantly changes the mending capability of materials. The healing behavior of the materials has been discussed on the basis of their thermal, mechanical, and rheological tests for each materials.

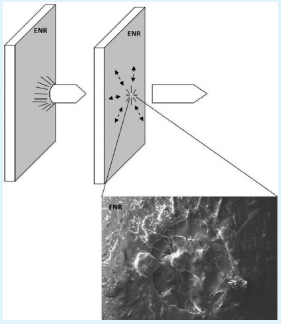


**KEYWORDS:** *ionomer, epoxidized natural rubber, self-repairing*

## INTRODUCTION

The development of autonomic repairing materials has surged a great deal of interest of scientific research in any field of materials science. The idea that autonomous repair is possible even in synthetic polymers has well proven its feasibility, and some solutions have already found important practical uses; many more applications are expected to benefit from the availability of these materials. Potential uses range from everyday objects, such as packaging for biomedicals and food, pressure and hazardous fluid containers, tires and inflatable components, to special applications such as space suits and living ambient or surface protections and aerospace structural components. In the aerospace field, in particular, damage management by the use of self-repairing materials is expected to lead to significant improvements in structures reliability and lifetime with respect to, or in conjunction with, structural monitoring and damage tolerance concepts.

Different approaches have been devised to engineer a material or a system with self-healing capability. Two important differences can be pointed out in the various approaches adopted to develop autonomic mending materials: one is actual self-repairing with no external action, another one is healing with interventions of external agents such as heat, pressure, radiation or flow of reactive substances. The goal of managing the damage is to maintain the primary functionality of materials, which is often related to their load carrying capacity, fluid tightness, or protective surface continuity. Many of such approaches have a remarkable resemblance to living tissues mechanisms, in that they possess the capability to recover, in total or partially, the original properties after damage by processes including the ability to sense damage,[1] deliver some healing agent to the damage zone[2] and/or providing heat,[3] light,[4] or other external stimuli for healing. On the other hand the complexity of these approaches often limits their efficiency and actual technical practicability. Among the different approaches, the development of intrinsically self-repairing materials assume a preeminent importance, as long as materials with selected properties are available for the specific applications.

The unique autonomous-repairing behavior of ionomers has been reported in several papers.[5−11] Ionomers are thermoplastic ionic polymers, e.g., hydrocarbon polymers bearing pendant carboxylic acid groups, that are either partially or completely neutralized with metal or quaternary ammonium ions.[12] Their mechanical properties are those typical of plastic materials, being relatively stiff and hard. The self-repairing phenomenon of ethylene-methacrylic acid copolymers partially neutralized with sodium (EMNa) or zinc (EMZn) was found to occur in different temperature conditions; their healing after high energy impact tests such as bullet penetration and low rate damage as in razor blade cutting or low speed punctures was investigated. On this basis, possible healing mechanisms for

**Received:** October 15, 2011
**Accepted:** November 16, 2011
**Published:** November 16, 2011

  

these materials were suggested. Composites with hard dispersed particles or nanoparticles also showed to retain at least partial self-healing properties.[5,6] In ionomeric materials, the presence of ionic clusters and the order-to-disorder transition phenomenon of the clusters have been related to healing effects.[7,13,14] However, intermolecular diffusion and thermally controlled reversible hydrogen bonding have been demonstrated to play a fundamental role; initial studies by Kalista et al.[5−7] reported a two-stage healing mechanism for ionomers by projectile puncture tests. This self-repairing mechanism was also supported by a newly developed quasi-static method by Varley and Van Der Zwaag.[8] Recently, the same researchers showed that the ultimate healing level depends on the elastic response during the impact and postfailure viscous flow.[9] They also reported the occurrence of consecutive healing events during high impact penetration of ionomers. It is worth to consider that studies by Fall[10] and Kalista[5] on the thermally activated healing of ionomer reported that the temperature of the impact zone during the bullet penetration reaches 120 °C, which is about 30 °C above the melting temperature of pure ionomer. The physical-cross-linking between acid functional groups and salt ions is thought to have influence on the healing mechanism and efficiency. Another important study by Vanhoorne[15] observed a significant influence of plasticization of ionic aggregates or acid-cation exchange mechanism on the melt-flow behavior of sodium and zinc containing methacrylic acid ionomers. The plasticizing effect of different acid groups on the self-healing behavior of ionomer has been studied by Varley et al.[11]

As a matter of facts, up to now, while extensive investigations are reported about ionomers, polymeric blends containing ionomers have found practically no attention by researchers, as healing behavior is concerned. In recent researches, the authors have investigated blends of EMNa with ethylene-vinylalcohol copolymer or with pure epoxidized natural rubber (ENR), showing that self-repairing capacity can be maintained in blends within defined composition ranges.[16,17] In this study, two different ion containing ionomers have been used to prepare blends with ENR and different chemical and physical properties have been investigated to understand their healability following a projectile damage.

In a number of applications, deformable elastomeric and self-repairing materials may greatly improve the performances; examples of such applications are packaging films, sealants and adhesives, impact absorbing layers, container walls or linears, industrial gloves, and inflatable space structures. Recently, synthetic elastomeric materials with self-mending capabilities related to microencapsulated healing agents have been studied.[18,19] The synthesis of autonomous-repairing rubber based on supramolecular assembly was reported by Cordier et al.,[20] and some synthetic, self-repairing products based on such a concept have reached the market stage.[21]

In this research, a different approach has been followed to develop polymeric materials with self-repairing capability and also with mechanical properties selectable over a wide range, from those typical of soft rubbers to those of hard plastics. Following such a strategy, a series of different ionomer/ENR blends have been prepared and characterized with two different ionomers based on poly(ethylene-co-methacrylic acid) partially neutralized with sodium or zinc salts. The self-repairing behavior of ENR and blends with ionomers has been investigated by ballistic puncture tests. The healing has been checked by both optical and scanning electron microscopy and also by depressurized air flow tests.

ENR is obtained from the partial epoxidation of the natural poly cis-isoprene molecules, resulting in a totally new type of elastomer. ENR molecule exhibits three different functionalities available for possible cross-linking, i.e., double bonds, epoxy, and acid groups in the main chain, while retaining most of the properties of natural rubber. The epoxide groups are randomly distributed along the natural rubber chain. The response of pure poly isoprene to ballistic puncture was also tested to investigate the effect of functionality on healing of rubber.

Remarkably different healing behavior was recorded in the different blends.[16,17] Unexpectedly all blends with epoxidized rubber and sodium-based ionomers showed full healing, while the blends with zinc based ionomers presented only partial repair. The dissimilar behavior is discussed on the basis of possible cross-linking between the epoxidized rubber and the ionomer during processing.

To better understand the role of functionalized rubbery phase in the self-repairing behavior of the blend, both ionomers were also blended with ENR in the presence of a free radical generator, dicumylperoxide (DCP), and thus producing materials with various degree of cross-linking of the rubbery phase. Rheological tests, along with the differential scanning calorimetric (DSC) analyses were carried out to investigate the viscoelastic behavior and thermal properties of blends and pure materials.

## EXPERIMENTAL SECTION

**Materials.** In this research, poly(ethylene-co-methacrylic acid) with 15% acid content, partially neutralized with sodium (EMNa) or zinc (EMZn) were purchased from Sigma-Aldrich as chemical products. Sodium content of 1.19% and zinc 1.27% were determined by elemental analysis, corresponding to about 26% of acid groups neutralized with sodium or 10% neutralized with zinc. Melt index values of used EMNa and EMZn are 2.8 g/10 min and 14.00 g/10 min (at 190 °C), respectively. Poly(cis-1,4-isoprene) from Aldrich was also used as received. The molecular weight of EMNa and EMZn were found to be $13.6 \times 10^4$ and $26.4 \times 10^4$ g/mol, respectively.

Epoxidized natural rubber (ENR-50) with a molecular weight of $3.9 \times 10^4$ was supplied by SAN-THAP International Company Ltd., Thailand. Mooney viscosity of 70−90 and glass transition temperature of −24 °C are reported by the producer. Dicumyl peroxide (DCP), used as a cross-linking agent for ENR, was purchased from Sigma-Aldrich.

**Determination of Epoxy and Carboxylic Acid Groups in ENR.** The epoxy groups content of ENR was measured according to ASTM D1652−04. A content of 4.5 mequiv for one gram of ENR was determined.

To evaluate the amount of carboxylic acid groups by potentiometric titration method, 500 mg of ENR were added into 30 mL of methylene dichloride. The solution of ENR was treated in ultra-sonicator for 1 min and this was repeated three times in order to increase the dissolution rate. After 3 days, 30 mL of ENR solution was transferred into a 100 mL separating flask. Twenty ml of aqueous tetrabutylammonium hydroxide of 0.14 M was then added to the solution. Afterward, the flask was shaken vigorously for several minutes; the nonfoaming and water containing phases were thus distinguished inside the flask. The flask was then kept in static condition for a few minutes and 10 mL of water was added for better separation of two phases. After this the water was removed and the residual methylene dichloride was separated by centrifuging. Back titration was performed with 0.1 M HCL. The carboxylic acid groups content measured was 0.62 mequiv for one gram of ENR. The value was taken as the average of three titrations of the sample. The results indicate that about 7 epoxy groups are present for any carboxylic acid group.

**Sample Preparation.** Pure ENR and polyisoprene were mixed with different amount of DCP (0.2, 0.5 and 0.8% by weight) in a discontinuous mixer, (Brabender Plastograph, Germany) at 100 °C; they were then compression molded and vulcanized at 160 °C for 12 min. Blends of EMNa/ENR and EMZn/ENR, with no DCP added, were melt-blended in the discontinuous mixer at 120 °C; rubber contents ranging from 15% to 50% were obtained. After the melt mixing, all blends were compression molded at 160 °C for few minutes to produce 2 ± 0.1 mm thickness plates. EMNa/ENR blends (30% and 50% rubber) with DCP added were also prepared by the same mixing procedure but with a compression molding time of 12 min.

**Ballistic Puncture Tests and Evaluation of Self-Repairing.** A first set of ballistic puncture tests on pure ionomers and their blends with ENR (with no DCP cross-linking agent) was performed at Fiocchi Munizioni Ballistic Lab. by shooting 4.65 × 19.2 mm bullets through 100 × 100 × 2 mm square plates at 23 °C and at a speed range of 703−730 m/s. The specimens were stored in a refrigerated container at −18 °C after the tests to avoid possible relaxation effects before the observations. A second set of tests on cross-linked polyisoprene, cross-linked ENR and its blends with EMNa ionomer was performed with 9 × 21 mm bullets at the Brescia Local Police Station shooting facility, although in such case actual bullet speeds could not be measured. Bullet speeds in the range 360 to 380 m/s are however estimated.

To check for the healing efficiency, we applied an initial pressure difference of 0.8 bar in a closed volume sealed in correspondence of the puncture zone by a vacuum pump. Air tightness through the hole was tested for a specified time (one hour) both by following vacuum decay and by checking for possible flow of a fluid droplet placed at the damage zone with the applied pressure difference. When the hole was healed, no appreciable vacuum decay was detected within the specified time range but for nonhealed samples vacuum decay was observed within a few seconds. A sketch of the experiment is depicted in Figure 1.

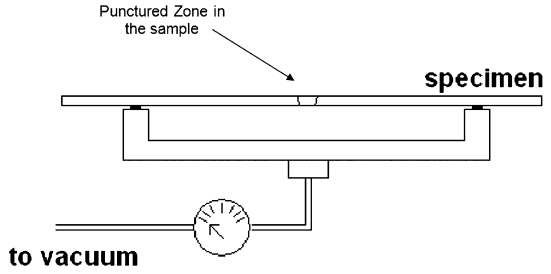


**Figure 1.** Set up for depressurized air-flow test.

**Evaluation of Morphology of the Punctured Zones.** All specimens were observed by optical stereomicroscope both in the bullet entrance and exit sides at 10−100× magnifications. Scanning electron microscopic (SEM) analyses were performed on the damaged surfaces of the specimens using a scanning electron microscope (LEO EVO 40). Samples were mounted with carbon tape on aluminum stubs and then sputter coated with gold to make them conductive prior to SEM observation.

**FTIR Analysis and Cross-Link Density Measurements.** The chemical structures of films were determined using Fourier transform infrared (FTIR-ATR (JASCO-300E)). The specimens were dried in a vacuum desiccator with $P_2O_5$ for 24 h before the experiment. The spectra of the blend films were recorded at a range of 4000−650 $cm^{-1}$ in absorbance mode. 256 scans at a resolution of 2 cm-1 were obtained and stored.

Apparent cross-link densities of the vulcanized ENR were measured at 20 °C by the swelling method. ENR samples were soaked in toluene for 2 days and the weight gain of the swollen samples was measured as function of time. The swelling ratio ($Q$) was calculated as $Q = (W_s - W_u)/W_u$, where $W_s$ and $W_u$ are the weights of the swollen and unswollen samples. The reciprocal swelling ratio ($1/Q$) at equilibrium was used as the apparent cross-link density.[22]

**Transmission Electron Microscopy (TEM).** The samples were microtomed at −80 °C using a Leica EM UC7 ultramicrotome with a Leica EM FC7 cryo chamber attachment. The sections were observed unstained in a transmission electron microscope (TEM) FEI CM120.

**Mechanical and Rheological Tests.** Tensile tests were performed by an Instron 3366 Dynamometer at 25 °C and at a cross-head rate of 10 mm/min. The thickness of the specimens was 2 ± 0.1 mm. ASTM D638 was followed for the tensile tests.

Dynamic mechanical tests were performed with a Rheometrics RDAII dynamic mechanical analyzer at 1 Hz frequency in a temperature range 20−110 °C. Rectangular torsion geometry was employed.

The measurement of complex shear viscosity of pure and blend materials was performed with parallel plate geometry (25 mm diameter) at different temperatures (120 to 180 °C) and in a frequency range of 0.5−50 Hz. Tests of viscosity change with time, at constant temperature, were also carried out to detect possible cross-linking variations.

**Differential Scanning Calorimetry (DSC).** Thermal analysis was performed in nitrogen atmosphere (50 mL/min) with a TA Instruments, DSC Q100, differential scanning calorimeter at a constant heating rate of 10 °C/min in the −50 to 120 °C temperature range for all blends and pure components. The Tg was taken as the inflection point of the heat capacity vs temperature curve, on the second heating scan, after cooling at 10 °C/min; the average of three tests at the same heating rate was considered.

## RESULTS AND DISCUSSION

**Self-Repairing Process of Epoxidized Natural Rubber and of Pure Ionomers.** A number of blends, consisting of EMNa or ENZn ionomers with different contents of pure or vulcanized ENR, were prepared and tested by ballistic tests. The healing of each material was observed by optical microscope and checked with air-flow tests after the ballistic puncture (Table 1). ENR (cross-linked with 0.2, 0.5, and 0.8 wt % of DCP) showed complete self-repairing after the bullet penetration (Figure 2a, b, 9 × 21 mm bullet). Also both the pure EMNa and EMZn showed complete self-repairing in ballistic puncture tests, as expected (Figure 2c,d, 4.65 × 19.2 mm bullet).

The self-repairing behavior of vulcanized ENR can give useful insight for the understanding of self-repairing mechanism involved in EMNa/ENR or EMZn blends. In fact, the self-repairing behavior of vulcanized ENR is quite different from that of ionomers, where viscoelasticity as well as recrystallization kinetics, are responsible of the healing process.[5]

The effect of cross-link density of vulcanized ENR (with 0.2−0.8 wt % DCP of ENR) on their healing behavior was also investigated. The variation in swelling ratio of vulcanized ENR at different time was measured up to equilibrium. Figure 3 shows the apparent cross-link density as a function of DCP content. It can be noticed that healing was independent of the cross-linking level determined for all vulcanized ENR in this study. Probably all these vulcanized ENRs maintained higher molecular flexibility at all cross-linking levels determined and thus, the fast recovery of extensive deformation along with instantaneous interdiffusion of macromolecular chain following a ballistic puncture facilitated the healing of ENR. Figure 4 shows a scanning electron micrograph of the punctured zone (9 mm bullet) of ENR vulcanized with 0.5 wt % DCP. The area around impact zone appears to be undeformed, because of the deformation recovery and the adhesion of dismantled surfaces resulting from the chain interdiffusion in the crater zone is also

**Table 1. Results of the Depressurized Air-Flow Tests for All Materials**

| pure components & blends | compositions (w/w) | pressure at the impact zone[a] (bar) | pressure drop/ failure (+)ve[b]/(−) ve[c] |
|---|---|---|---|
| pure EMNa | | 0.8 | (−)ve |
| pure EMZn | | | (−)ve |
| ENR (0.2 wt % DCP) | | | (−)ve |
| ENR (0. Five wt % DCP) | | | (−)ve |
| ENR (0.8 wt % DCP) | | | (−)ve |
| EMNa/ENR | 85/15 | 0.8 | (−)ve |
| EMNa/ENR | 80/20 | | (-)ve |
| EMNa/ENR | 70/30 | | (−)ve |
| EMNa/ENR (0.5 wt % DCP) | 70/30 | | (−)ve |
| EMNa/ENR | 50/50 | | (−)ve |
| EMNa/ENR (0.5 wt % DCP) | 50/50 | | (−)ve |
| EMZn/ENR | 85/15 | 0.8 | (+)ve |
| EMZn/ENR | 80/20 | | (+)ve |
| EMZn/ENR | 70/30 | | (+)ve |
| EMZn/ENR | 50/50 | | (+)ve |

[a]This pressure (0.8 bar) was maintained for 1 h at the impact zone. [b]Pressure drop is positive ((+)ve) when the impact zone cannot maintain the imposed pressure for a few seconds because of incomplete hole closure. [c]Pressure drop is negative ((−)ve) when the impact zone maintains the imposed pressure in the impact zone for the specified time (i.e., 1 h) because of the complete hole closure.

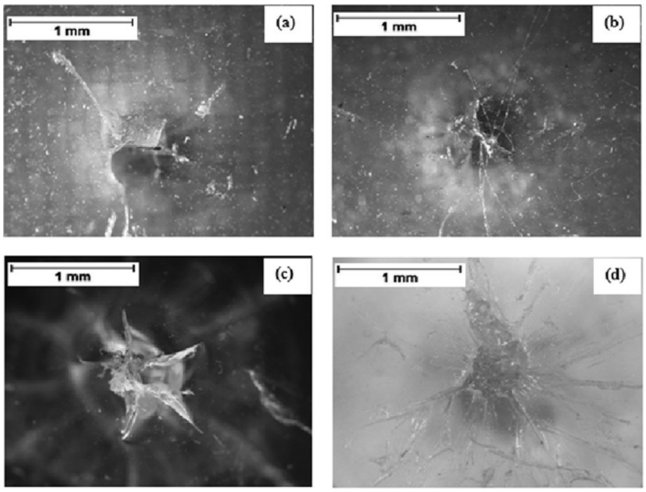


**Figure 2.** Optical micrographs of bullet impact zones (exit zones) of ENR vulcanized with (a) 0.2 wt % DCP and (b) 0.5 wt % DCP (c); pure EMNa and (d) pure EMZn.

evident. The adhesion phenomenon is not only influenced by the chain interdiffusion process but also the intermolecular interaction in the macromolecules.[23] This was why the self-healing behavior of a synthetic polyisoprene (cis-1,4-polyisoprene) cross-linked with DCP in the same conditions was also tested. No healing was observed for vulcanized polyisoprene even if its $T_g$ (−63 °C) is lower than the Tg of ENR (−20 °C). Temperature activated epoxide ring-opening reaction and formation of ester linkages with carboxylic acid groups in ENR[24] following the bullet penetration can possibly give an important contribution to the self-healing of the rubber.

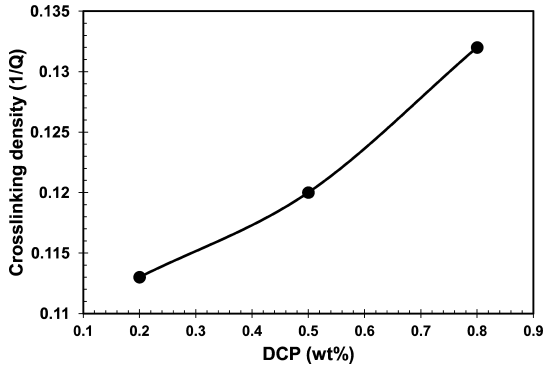


**Figure 3.** Reciprocal swelling ratio $1/Q$ of ENR vulcanized by 0.2, 0.5, and 0.8 wt % DCP. Apparent cross-linking density was measured at equilibrium swelling.

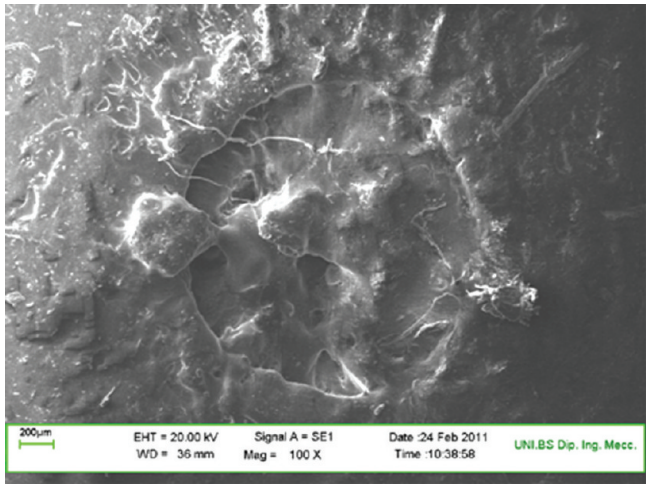


**Figure 4.** SEM image of punctured zone of vulcanized ENR+0.5% DCP.

This suggests that the presence of epoxy and acid groups in ENR play an important role in healing such high energy impact damage. Thus the healing in ENR is accompanied by shape recovery as well as the adhesion of the dismantled surfaces following the bullet penetration.

The existence of functional groups (e.g., epoxy and carboxylic acid) in ENR was detected by FTIR spectroscopy and by potentiometric titration. Figure 5a shows the comparison between the chemical structures of ENR and Polyisoprene. Possible interactions among functional groups in Ionomers/ENR blends have been investigated by FTIR and this has been discussed later.

**3.2. Self-Repairing Process in Blends.** Microscope observations and healing tests after bullet punctures (4.65 mm bullets) confirmed complete self-repairing for all the compositions of EMNa/ENR blends; on the contrary, only partial self-repairing phenomena (referring to the reduced diameter of punctured zones) were observed in different compositions of EMZn/ENR blends. Figure 6 shows the optical micrographs of bullet impact zones of 15 to 50 wt % EMNa/ENR blends.

Figure 7 shows the optical micrographs of the punctured zones for EMZn/ENR blends containing 15 to 50 wt % ENR. Brittle fracture surfaces were observed in the punctured zones of all compositions and depressurized air flow tests confirmed the evidence of incomplete healing for blends with EMZn

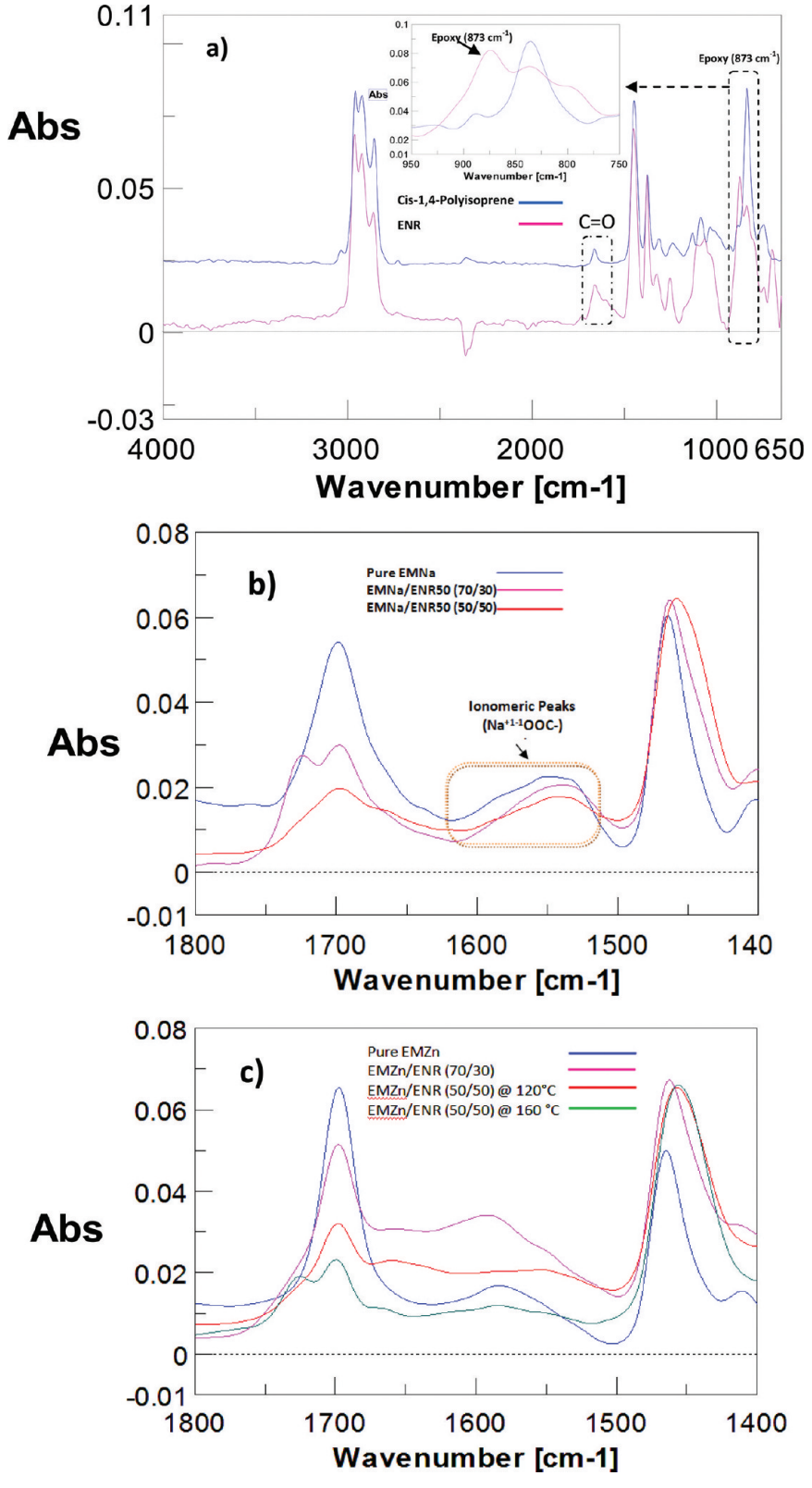


**Figure 5.** FTIR spectra of (a) pure ENR and PISP, (b) EMNa/ENR and (c) EMZn/ENR blends.

(Table 1). However, the diameter of the holes remarkably reduced, thus evidencing extensive viscoelastic recovery, but to a lower extent than EMNa blends. The reason for such incomplete healing can be better justified by FTIR analysis.

The chemistry of the blends containing EMNa and EMZn is highly influenced by the availability of free acid group as well as the type of cations present in the matrix. EMNa contains a monovalent cation, i.e., sodium ion ($Na^+$), whereas EMZn contain divalent zinc cations ($Zn^{2+}$). Usually, the divalent cations produce bridge between two carboxylate ions forming different coordinated complexes and the monovalent cations create dipole−dipole interactions between the salt ion


dx.doi.org/10.1021/am201417h | ACSAppl. Mater. Interfaces 2011, 3, 4865−4874

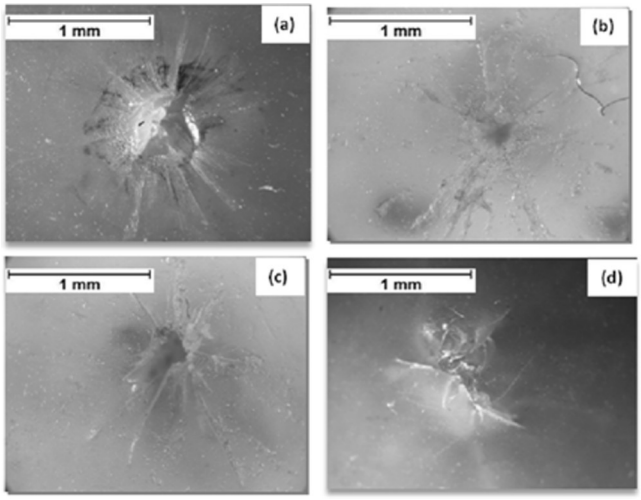


**Figure 6.** Optical micrographs of bullet impact zones (exit zones) of self-healed EMNa/ENR blends containing (a) 15, (b) 20, (c) 30, and (d) 50 wt % ENR.

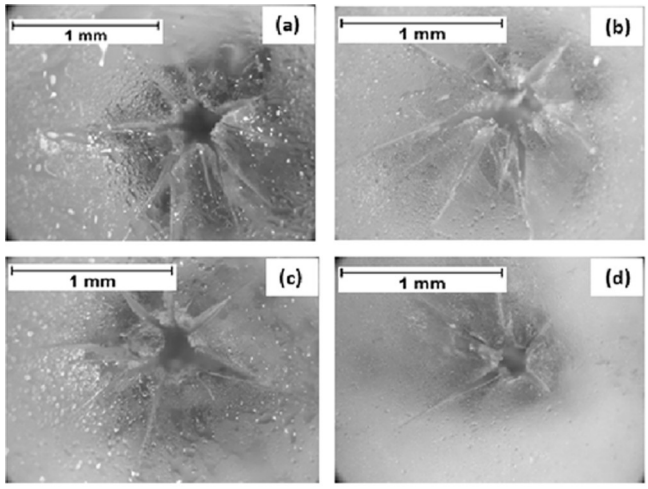


**Figure 7.** Optical micrographs of bullet impact zones (exit zones) of nonhealed EMZn/ENR blends containing (a) 15, (b) 20, (c) 30, and (d) 50 wt % ENR.

pairs.[25,26] The formation of different complex structures is also dominated by the acid group environment.[27] Panels b and c in Figure 5 show the FTIR spectra of EMNa/ENR and EMZn/ENR blends, respectively. The absorption peak at 1700 $cm^{-1}$, corresponding to the unneutralized carboxylic acid group, shows decrease in intensity with increasing ENR content. In addition to this, the absorption peaks in the region of 1620–1598 $cm^{-1}$ are associated with the carboxylate ion peaks (also known as the region associated with neutralized and associated acid groups[27]), and the positions of these peaks are slightly affected by the ENR content. Slight shift of this peak to higher wavenumber can be observed for higher ENR content of the blends. On the other hand, the absorbance corresponding to the neutralized and associated acids (1650–1550 $cm^{-1}$) in the EMZn/ENR blends is highly influenced by ENR content. Significant shifts of these peaks have been observed. Such shifts should be associated with the formation of more coordinated complexes by $Zn^{2+}$ ions in the matrix because of the availability of more acid groups of ENR in the matrix. Moreover, there exist possible interactions between unneutralized acid groups of EMZn and epoxy group of ENR. The formation of ester group in the blends could not be detected possibly due to a lower amount of ester formed at the blending temperature used (i.e., 120 °C). However, another blend (EMZn/ENR) containing 50 wt % ENR was prepared at 160 °C to have the evidence of ester formation[25] in the blend, which was confirmed by FTIR. Thus the healing in EMZn/ENR blends is influenced by the rearrangement of coordinated complexes of $Zn^{2+}$ ions and chemical interaction between acid and epoxy groups of EMZn and ENR, respectively. The rearrangement of coordinated complexes should promote higher physical cross-linking by $Zn^{2+}$ ions and the existence of chemical interaction between EMZn and ENR should not be excluded. This is why the morphology of EMZn/ENR blends is different from that of EMNa/ENR blends, as indicated by SEM and DSC analysis. The morphology of the impact zones gives useful information about the microstructure of the healing phases. Figure 8 shows the SEM images of the impact zones for both healed and nonhealed blends. It is evident from Figure 8a that the healing occurs at the intermediate zones where the mobility of ENR phase is less dominated by EMNa phase. This mobility is still maintained even in the blends containing DCP (Figure 8c). On the other hand, a different morphology can be observed in the punctured zone of EMZn/ENR (50/50) blend, where the mobility of ENR phase is restricted due to the interaction between EMZn and ENR macromolecular segments, as discussed earlier. In addition to this, fine dispersion of rubber particles (20–50 $\mu$m in diameter) can be recognized in the vicinity of punctured zone, which indicates that surface morphology is predominantly influenced by ENR phase. Moreover, the inner surface in the crater zone of EMNa/ENR blend is smoother than the surface crater of EMZn/ENR blend. The ductile tearing at the inner surface along with stress induced fibrillated morphology at the edge of the puncture zone can be recognized in EMZn/ENR blend. The evidence of smoother surface in EMNa/ENR blends indicates a complete stress relaxation of the material because of the higher mobility of ENR phase following the puncture damage. Although the type of ion content dominates the morphology of blends as well as the healability of the materials, the coexistence of two incompatible but healable phases in EMNa/ENR blends certainly influences the healing of the materials. The phase structure as well as their influence on the overall thermal properties of the blends can be investigated by DSC.

The TEM micrographs of EMNa/ENR give useful information about the composition dependent changes in the phase morphology of the blends and their effect on the self-repairing behavior. Figure 9a and 9b show the morphology of 15 and 50 wt % ENR containing EMNa/ENR blends, respectively. It can be noticed that, in 15 wt % ENR containing EMNa/ENR blends, the dispersed phase is ENR and rubber particles are finely distributed with an average size of 1.40 $\mu$m. However, phase transition has been observed for the 50 wt % ENR containing EMNa/ENR blend, where cocontinuity of both EMNa and ENR phases is evident. Thus, the healing in EMNa/ENR blends with lower ENR content is highly influenced by the EMNa phase, whereas for the 50/50 (EMNa/ENR) blend, the contribution of both phases is supposed to affect the healing of the materials following the damage.

Complete hole closure requires welding of damage zone, which is related to thermal behavior of the material. DSC was used to investigate the thermal behavior of the blends,

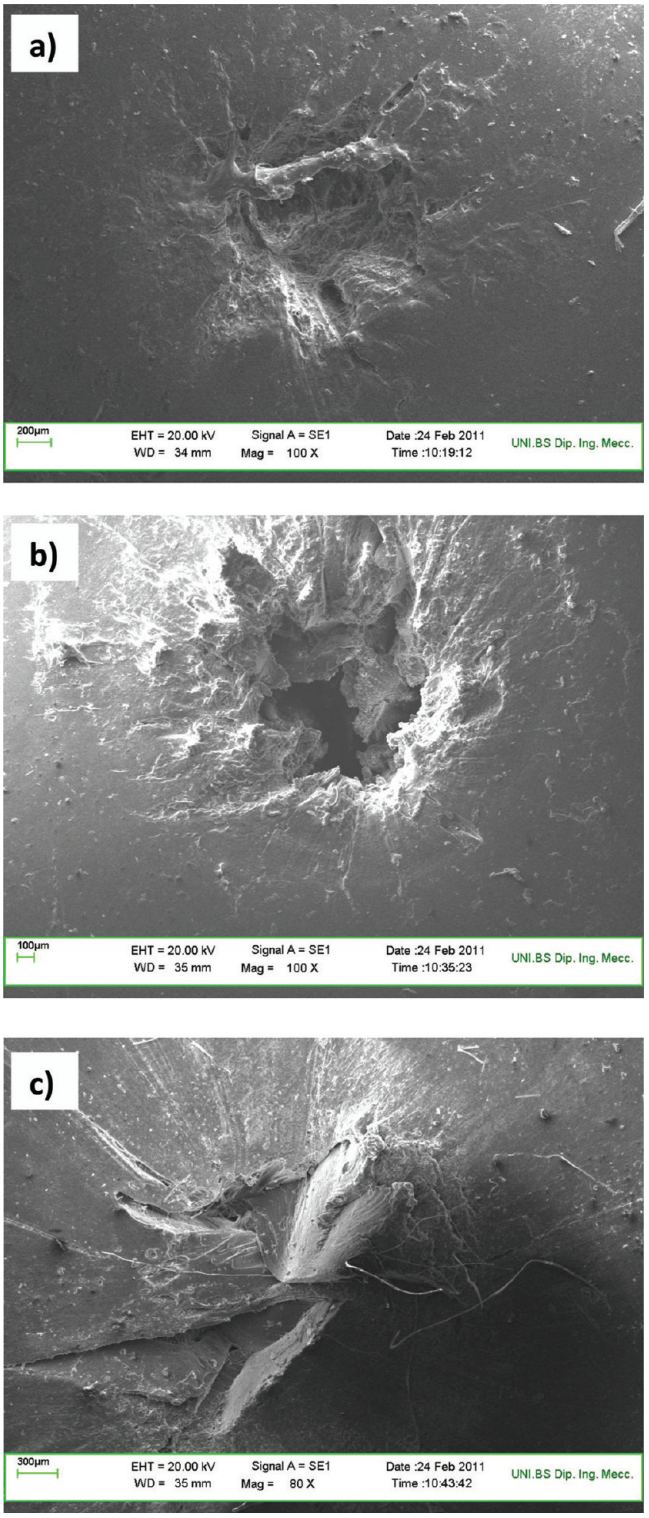


**Figure 8.** SEM images of impact zones of (a) EMNa/ENR (50/50); (b) EMZn/ENR (50/50); and (c) EMNa/ENR (50/50) with 0.5% DCP.

suggesting the effect that the puncture-repairing event may have on the thermal history of the polymers. Tables 2 and 3 summarize different thermal properties for both EMNa/ENR (with and without DCP) and EMZn/ENR blends or ENR (vulcanized and unvulcanized). EMNa/ENR blends show only a single melting peak and two different $T_g$ values (Table 2): one well below room temperature, consistent with the rubber phase,

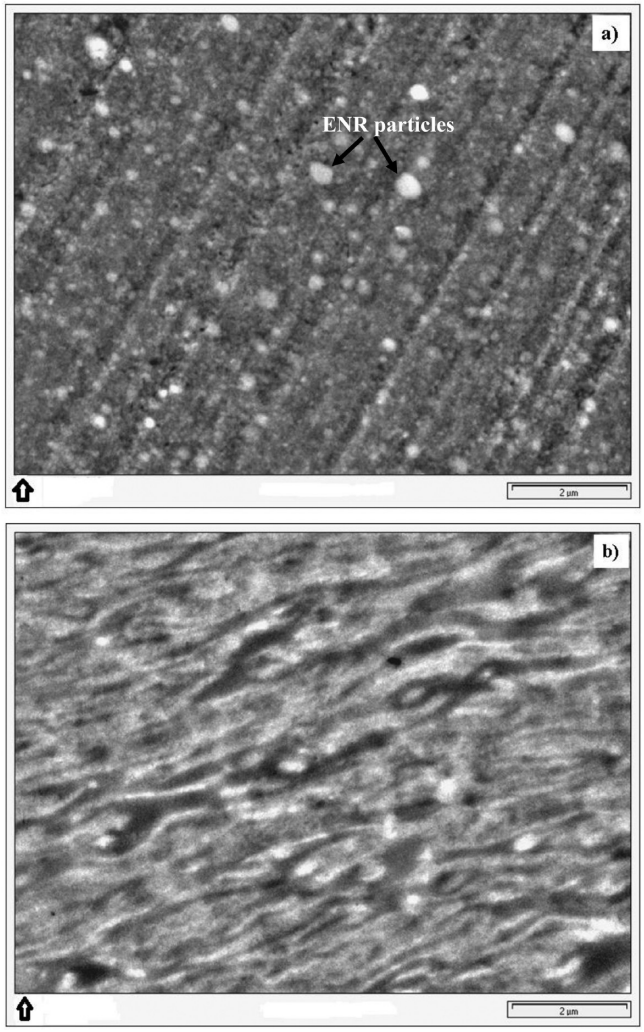


**Figure 9.** TEM micrographs showing composition dependent phase morphologies in (a) 15 and (b) 50 wt % ENR containing EMNa/ENR blends.

**Table 2. Thermal Properties of Pure EMNa, ENR, and EMNa/ENR Blends**

| EMNa/ENR (wt %) | DCP (wt %) | $T_g$ (°C) first | $T_g$ (°C) second | $T_m$ (°C) | $\Delta H$m (EMNa phase)[a] (J/g) |
|---|---|---|---|---|---|
| 100/0 | 0 | | 51.0 | 95.4 | 26.4 |
| 85/15 | 0 | −20.0 | 51.0 | 94.0 | 62.7 |
| 80/20 | 0 | −18.0 | 51.0 | 93.4 | 50.8 |
| 70/30 | 0 | −20.0 | 51.0 | 93.3 | 45.3 |
| 70/30 | 0.2 | −19.7 | 47.6 | 94.4 | 43.3 |
| 70/30 | 0.5 | −18.7 | 47.5 | 93.9 | 47.0 |
| 50/50 | 0 | −20.0 | 51.0 | 93.0 | 56.0 |
| 50/50 | 0.2 | −19.8 | 47.8 | 93.9 | 47.4 |
| 50/50 | 0.5 | −20.0 | 48.3 | 94.8 | 18.8 |
| 0/100 | 0 | −20.0 | - | - | - |
| 0/100 | 0.2 | −20.4 | - | - | - |
| 0/100 | 0.5 | −20.2 | - | - | - |

[a]Enthalpy normalized over EMNa content.

and another at about 50 °C, consistent with ionomeric phase, thus evidencing heterogeneous phase structure of EMNa/ENR blends (Figure 10). The $T_g$ of ENR phase remains unaffected


dx.doi.org/10.1021/am201417h | ACSAppl. Mater. Interfaces 2011, 3, 4865−4874

**Table 3. Thermal Properties of Pure EMZn and EMZn/ENR Blends**

| EMZn/ENR (wt %) | $T_g$ (ENR phase) (°C) | $T_m$ (°C) | $\Delta H$ (EMZn phase)[b] (J/g) |
|---|---|---|---|
| 100/0 | | 91.6 | 89.5 |
| 85/15 | | 85.9 | 61.7 |
| 80/20 | | 84.7 | 66.0 |
| 70/30 | −17.0 | 83.4 | 55.4 |
| 50/50 | −19.0 | 85.1 | 31.8 |
| 0/100 | −20.0 | | |

[b]Enthalpy normalized over EMZn content.

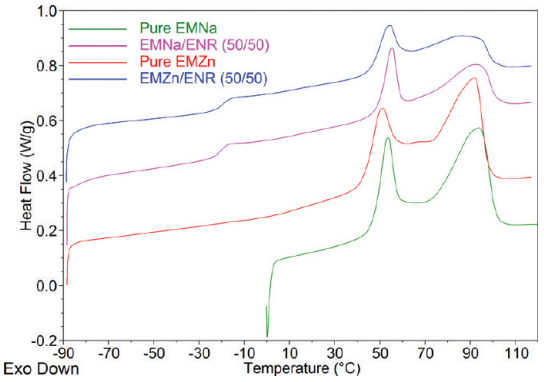


**Figure 10.** Phase morphology of EMNa/ENR and EMZn/ENR blends observed by DSC thermograms in first heating scan.

by the compositions in the blends. A negligible depression of melting point was observed for these blends and a constant degree of crystallinity of EMNa phase in the blends is maintained. However, a remarkably higher melting enthalpy compared to pure ionomer was observed, indicating easier crystallization of EMNa as consequence of ENR presence.

In addition, ENR vulcanized with 0.2−0.8 wt % DCP shows $T_g$ values close to the unvulcanized ENR. Similar $T_g$ values of ENR with or without DCP were also observed in blends with $Na^+$-based ionomer. However, the presence of higher amount of DCP (0.5 wt %) promotes some grafting reaction between EMNa and ENR and thus reducing the crystallinity in the blends. This is in consent with the lower value of $\Delta H$ presented by 0.5 wt % DCP containing blends, indicating a lower degree of crystallinity in comparison with pure EMNa and other blends.

Interestingly, in EMZn/ENR blends, the $T_g$ values for ENR phase increased with the increase of EMZn content (Table 3). This observation confirms that cross-linking by epoxy functionalities can effectively occur between EMZn and ENR at the processing conditions, leading to a significant reduction molecular mobility. On the other hand, for EMZn/ENR blends, a second $T_g$ above room temperature was not observed in second heating scan for all compositions (Table 3). A broad fusion peak was observed possibly because of the lower mobility of macromolecular chains that produce crystalline phases with higher defects and/or crystals with lower dimension in the blends. Moreover, although melting enthalpy is consistently higher than with EMNa, in EMZn blends, a steady decrement was observed with increasing ENR content; this is opposite to what occurs in EMNa/ENR blends.

The rheological behavior of ENR and blends can give some useful information regarding molecular mobility and possible interactions between ionomers and ENR. Complex viscosity measurements of EMNa blends with pure ENR showed that viscosity of the blends significantly increases with time at temperature above 160 °C (Figure 11). This indicates that a

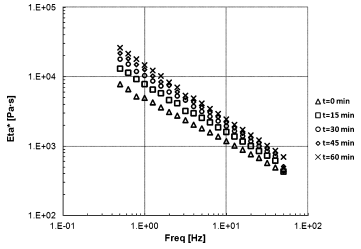


**Figure 11.** Complex viscosity of EMNa/ENR (70/30) maintained at 180 °C for different times.

reaction between EMNa and ENR can effectively occur, although to a limited extent at the processing conditions employed.

Similar viscosity tests conducted with pure ENR and ENR with DCP showed no evidence of viscosity change with time. Moreover, the complex viscosity of rubber appears only slightly affected by DCP addition (Figure 12); this fact, together with

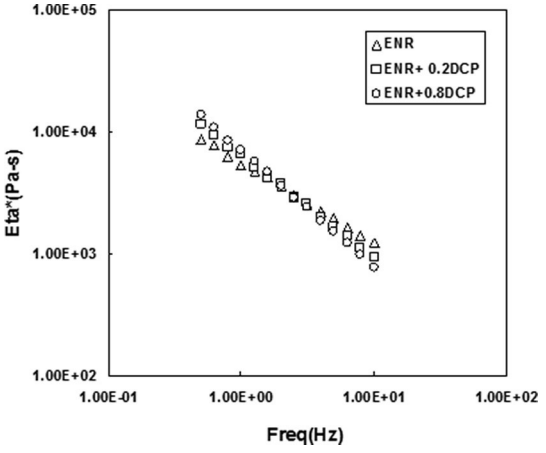


**Figure 12.** Complex viscosity of pure ENR and vulcanized ENR.

the negligible variation of $T_g$, indicates the maintenance of high mobility of macromolecular chains in ENR also in the vulcanized form.

Figure 13 reports the measured mechanical properties of the blends. As expected, the addition of soft rubber induces a marked reduction in elastic modulus and strength in comparison with the pure ionomers. The decrement is higher for EMZn/ENR blends than that of EMNa/ENR blends; moreover, the addition of DCP in EMNa/ENR blends improves both modulus and strength in comparison with the samples not containing DCP.

## CONCLUSIONS

Two different blend series, EMNa/ENR and EMZn/ENR, were prepared by melt-mixing. The self-repairing behavior was investigated by a ballistic puncture tests. The optical/SEM micrographs and depressurized air flow tests confirmed the complete self-repairing behavior for all compositions of EMNa/ENR blends. Also, pure ENR shows self-repairing behavior in the same experimental conditions. On the other hand, self-repairing was not observed for all the compositions of EMZn/


dx.doi.org/10.1021/am201417h | ACSAppl. Mater. Interfaces 2011, 3, 4865−4874

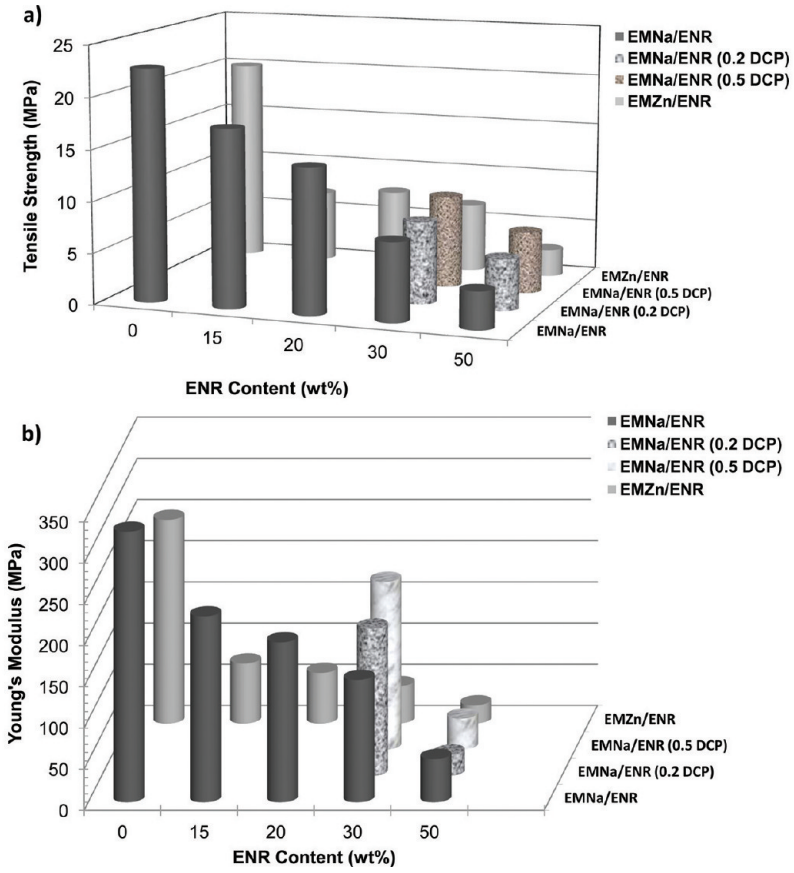


**Figure 13.** Effect of ENR content on (a) tensile strength (TS) and (b) Young's modulus of both blend series.

ENR blends because of the rearrangement of coordinated complexes of $Zn^{2+}$ ions and the existence of some level of chemical interaction between acid groups of EMNa and epoxy group of ENR. In case of EMNa blends, such reaction appears to occur at remarkably lower rate. ENR cross-linked by DCP does not significantly affect the molecular mobility of ENR, allowing it to preserve the self-healing capability also in the vulcanized form.

The availability of blends with physical and mechanical properties modulated over a wide range, yet maintaining efficient self-repairing behavior, remarkably extends the potential application areas of such materials.

## AUTHOR INFORMATION

### Corresponding Author

*E-mail: luca.dilandro@polimi.it.

## ACKNOWLEDGMENTS

The authors wish to thank Mrs V. Ferrari for her assistance in SEM observations. The contributions of Prof. Janszen, Mr. Bruno Romano of the Brescia Local Police Dept., as well as the Fiocchi Ammunitions Lab in performing ballistic tests is also gratefully acknowledged.

## REFERENCES

(1) Kolmakov, G. V.; Revanur, R; Tangirala, R; Emrick, T; Russell, T. P.; Crosby, A. J.; Balaz, A. C. *ACS Nano* **2010**, *4*, 1115−1123.
(2) Mauldin, T. C.; Rule, J. D.; Sottos, N. R.; White, S. R.; Moore, J. S. *J. R. Soc. Interface.* **2007**, *4*, 389−393.
(3) Chen, X.; Dam, M. A.; Ono, K.; Mal, A.; Shen, H.; Nutt, S. R.; Sheran, K.; Wudl, F. A. *Science* **2002**, *295*, 1698−1702.
(4) Ghosh, B; Urban, M. W. *Science* **2009**, *323*, 1458−1460.
(5) Kalista, S; Ward, T. C. *J. R. Soc. Interface* **2007**, *4*, 405−411.
(6) Kalista, S; Ward, T. C.; Oyetunji, Z. *Mech. Adv. Mater. Struct.* **2007**, *14*, 391−397.
(7) Varley, R. Ionomer as Self healing Polymers. In *Self Healing Materials: An Alternative Approach to 20 Centuries of Materials Science*, 1st ed.; Van Der Zwaag, S.; Springer: Dordrecht, The Netherlands; 2007, p 95−114.
(8) Varley, R. J.; Van Der Zwaag, S. *Acta Mater.* **2008**, *5*, 5737−5750.
(9) Varley, R. J.; Van Der Zwaag, S. *Polym. Int.* **2010**, *59*, 1031−1038.
(10) Fall, R. A.; , Puncture Reversal of Ethylene Ionomers − Mechanistic Studies. Master's Thesis, Virginia Polytechnic Institute and State University, Blacksburg, VA, 2001.
(11) Varley, R. J.; Shen, S; Van Der Zwaag, S. *Polymer* **2010**, *51*, 679−686.
(12) Holiday, L. *J Polym Sci: Polym Lett.* **1976**, *14*, 114−115.
(13) Eisenberg, A; Hird, B; Moore, R. B. *Macromolecules* **1990**, *23*, 4098−4107.
(14) Tadano, K; Hirasawa, E; Yamamoto, H; Yano, S. *Macromolecules* **1989**, *22*, 226−233.
(15) Vanhoorne, P; Register, R. A. *Macromolecules* **1996**, *29*, 598−604.
(16) Penco, M; Rahman A., Md.; Spagnoli, G; Jansen, G; Di Landro, L. *Mater. Lett.* **2011**, *65*, 2107−2110.
(17) Rahman A., Md; Penco, M; Spagnoli, G; Grande, A. M.; Di Landro, L. *Macromol. Mater. Eng.* **2011**, *296*, 000−000, DOI: 10.1002/mame.201100056.
(18) Keller, M. W.; White, S. R.; Sottos, N. R. *Adv. Funct. Mater.* **2007**, *17*, 2399−2404.
(19) Cho, S. H.; Andersson, H. M.; White, S. R.; Sottos, N. R.; Braun, P. V. *Adv. Mater.* **2006**, *18*, 997−1000.
(20) Cordier, P; Tournilhac, F; Soulié-Ziakovic, C; Leibler, L. *Nature* **2008**, *451*, 977−980.
(21) Reverlink, http://www.arkema.com.

(22) Choi, S. S.; Kim, J. C.; Ko, J. E.; Cho, Y. S.; Shin, W. G. *J. Ind. Eng. Chem.* **2007**, *13*, 1017−1022.
(23) Voyutskii, S. S.; Margolina, L. Yu. *Usp. Khim.* **1949**, *18*, 449−461.
(24) Poh, B. T.; Lee, K. S. *Eur. Polym. J.* **1994**, *30*, 17.
(25) Mohanty, S.; Nando, B. G. *Polymer.* **1997**, *38*, 1395−1402.
(26) Coleman, M. M.; Lee, J. Y.; Painter, P. C. *Macromolecules* **1990**, *23*, 2339.
(27) Walter, M. R.; Sohn, E. K.; Winey, I. K.; Composto, J. R. *J. Polym. Sci., Part B: Polym Phys.* **2002**, *41*, 2833−2841.